ELSEVIER

Composites Science and Technology 62 (2002) 1895–1912

COMPOSITES SCIENCE AND TECHNOLOGY

www.elsevier.com/locate/compscitech

Spring-in and warpage of angled composite laminates

Carolyne Albert, Göran Fernlund*

Metals and Materials Engineering, The University of British Columbia, Vancouver, BC, V6T 1Z4, Canada

Received 15 October 2001; received in revised form 14 June 2002; accepted 14 June 2002

Abstract

The residual stresses that develop in fibre-reinforced laminates during autoclave processing while the laminate is confined to the process tool often lead to dimensional changes such as spring-in of angles and warpage of flat sections. A large number of experiments were performed to examine the effect of design and process parameters on spring-in and warpage of composite laminates with a symmetrical lay-up. The parameters studied include part angle, thickness, lay-up, flange length, tool material, tool surface, and cure cycle. This paper shows that both design and process parameters can have a significant effect on spring-in and warpage and that there are interactive effects between them. The paper also shows that spring-in of angled laminates is sensitive to the measurement technique as the measured spring-in often is compounded by warpage of flat laminate sections. © 2002 Elsevier Science Ltd. All rights reserved.

Keywords: A. Polymer-matrix composites; Autoclave processing; C. Residual stress

1. Introduction

During autoclave processing of fibre-reinforced polymer composite structures there is an inevitable build-up of residual stresses, mainly due to differential thermal expansion between fibres and matrix, which often causes distortions of the fully cured structure. For the simple L and C geometries studied here, these distortions can be classified as warpage, or curving of initially flat sections, and spring-in, or a reduction of enclosed angles of angled sections. Spring-in will routinely occur in angled autoclave processed parts whereas warpage may or may not be an issue, depending on the design of the structure and the process conditions. Spring-in causes problems in assembly because of poor fit-up to mating structures and is typically compensated for when designing the process tooling using an experience based compensation factor. The absolute magnitude of the spring-in, however, is difficult to predict and is often variable in production. Fig. 1 shows a schematic of the effect of spring-in of a spar flange on the fit-up of fastener locations between a spar and a wing skin. Any warpage (curvature) of the spar flange or wing-skin would exacerbate the fit-up problem. To quantify process-induced deformation for simple geometries such as the spar shown in Fig. 1, the concept of a spring-in angle is commonly used. However, as will be demonstrated in this paper, spring-in angles are often not sufficient to quantify process-induced deformations as the deformation is often compounded by warpage of flat sections.

Spring-in is not only affected by the differential thermal expansion between the fibres and the matrix, but also by the evolution of mechanical properties of the laminate during processing. While fibre properties remain essentially constant, resin properties change dramatically throughout the cure cycle as the resin polymerizes. The development of residual stresses is dependent on the processing history because of the large changes in mechanical and physical properties during cure. Thus, spring-in, which is the result of residual stresses developing while the composite part is confined to the process tool, depends on the timing of events during processing.

Many parameters are known or suspected to affect spring-in [1–12] and it is convenient to classify them as intrinsic or extrinsic parameters. Intrinsic parameters are here defined as parameters related to part geometry and material properties, whereas extrinsic parameters are defined as parameters related to tooling and processing.

* Corresponding author. Tel.: +1-604-822-3673; fax: +1-604-822-3619.

E-mail address: goran.fernlund@ubc.ca (G. Fernlund).

0266-3538/02/$ - see front matter
PII: S0266-3538(02)00105-7

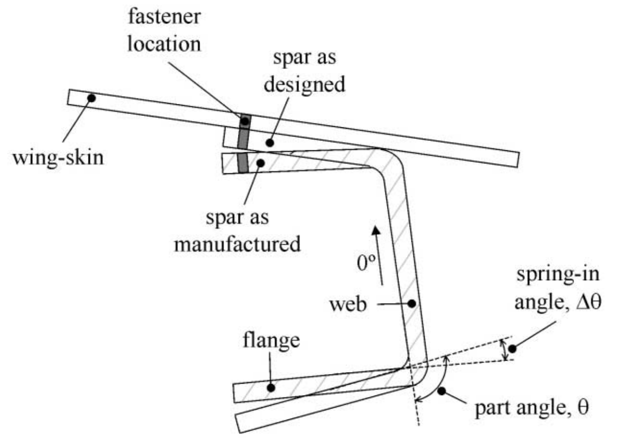

Fig. 1. Schematic of a typical spar/wing-skin assembly.

1.1. Effect of intrinsic parameters on spring-in

A simple equation [Eq. (1)] has been proposed for predicting spring-in of angled laminates based on material anisotropy [1,2]. This equation accounts for the temperature difference between cure and ambient conditions, the anisotropy of thermal expansion and cure shrinkage, and the part angle Fig. 1.

$$\Delta\theta = \Delta\theta_{\mathrm{CTE}} + \Delta\theta_{\mathrm{CS}} = \theta\left(\frac{(\alpha_l - \alpha_t)\Delta T}{1 + \alpha_t \Delta T}\right) + \theta\left(\frac{\phi_l - \phi_t}{1 + \phi_t}\right) \quad (1)$$

where: $\Delta\theta$ = spring-in angle; $\Delta\theta_{\mathrm{CTE}}$ = thermal component of the spring-in angle; $\Delta\theta_{\mathrm{CS}}$ = cure shrinkage component of the spring-in angle; θ = part angle; α_l = longitudinal coefficient of thermal expansion; α_t = through thickness coefficient of thermal expansion; ΔT = difference between cure temperature and ambient temperature; ϕ_l = longitudinal cure shrinkage; ϕ_t = through-thickness cure shrinkage.

The first term of Eq. (1), $\Delta\theta_{\mathrm{CTE}}$, is the thermal expansion anisotropy component, which is the result of residual stresses that develop during cool-down, when the laminate is fully cured. The second term, $\Delta\theta_{\mathrm{CS}}$, is the result of resin cure shrinkage and is associated with stresses that build up earlier in the cure cycle, as the material cures. Published results indicate that Eq. (1) in some cases provides a reasonable estimate of spring-in [3,4]. However, Eq. (1) does not account for extrinsic parameters such as tooling effects.

There is disagreement of the effect of corner radius on spring-in in the literature. One study indicates that spring-in is smaller for smaller radii [5]. Other studies have concluded that corner radius has little effect on the overall spring-in [6,7]. The effect of part thickness on spring-in is also unclear. While some studies have found that thinner parts have greater spring-in than thicker ones [5,8], other studies [6,7] revealed little difference. In contrast to these findings, one study found that doubling the part thickness increased the spring-in by over 20% [9]. The differences between these findings suggest that the effect of thickness on spring-in may be sensitive to other interacting parameters.

It has been reported that ply orientation has little effect on spring-in when comparing cross-ply, angle-ply and quasi-isotropic laminates [6,9]. It is generally agreed that spring-in is virtually zero for 90° lay-ups [6,9], whereas there is disagreement regarding the magnitude of spring-in of 0° lay-ups. With reference to Fig. 1, a 90° lay-up is here defined as one where all the fibres are oriented along the length axis of the spar, whereas a 0° lay-up is one where all the fibres are in the plane of the spar cross-section. While one study [9] showed that 0° laminates gave the highest spring-in, other studies [3,6,10] found that spring-in of 0° laminates is lower than that of multidirectional laminates.

For symmetrical laminates, the stacking sequence has been found to have little effect on spring-in [6]. The study noted that even when 0° and 90° plies were interchanged, spring-in remained virtually unaffected, provided that the lay-up remained symmetrical. In an experimental and numerical study [10], C-shaped parts were found to have greater spring-in than L-shaped parts. This difference was explained in terms of a possible 'geometric locking' of the C-shaped parts on the inner mould line that was not present with the L-shaped parts.

1.2. Effect of extrinsic parameters on spring-in and warpage

Spring-in due to thermal strain anisotropy is believed to be proportional to the difference between the cure temperature and the ambient temperature, see Eq. (1). However, this is not the only source of spring-in. The effect of cure temperature on the development of residual stresses has been studied. One study found that by processing at a lower temperature for a longer time, or by utilizing an intermediate lower temperature dwell in three step cure cycles, residual stresses can be reduced by as much as 30% [13]. However, processing at lower temperatures requires longer curing times. The same study showed that for a given cure temperature, reducing the cure cycle time can reduce residual stresses, resulting in a decrease of warpage of as much as 60%. However, reducing the cure time does not allow the curing reaction to complete which has a detrimental effect on the mechanical properties. A reduction of 12% in residual curvature was reported for asymmetric laminates when cooled down at a rate of 0.56 °C/min compared to a rate of 5.6 °C/min [13]. This was explained by viscoelastic stress relaxation being more significant for the slower cool-down. The same researchers also reported that varying the cool-down pressure from 0.35 to 1.0 MPa has no noticeable effect on warpage. In contrast, other work has shown that if a 2-hold cure cycle, with a first lower temperature hold and a second higher temperature hold, is designed such that the resin gels during the first temperature hold, spring-in can be significantly increased compared to a single-hold cure cycle [10,11]. The effect of cure cycle on thickness and fibre volume fraction distribution has been studied experimentally and numerically [24]. The study showed that by optimizing the cure cycle, the quality and strength of the part was enhanced.

A numerical study [12] indicated that reduction of the mechanical interaction between the part and tool at the tool-part interface reduces the spring-in angle. In the same numerical study, the tooling material was predicted to have a major effect on spring-in, with Invar tooling giving lower spring-in than aluminum tooling. Another numerical study [7] showed that the tool coefficient of thermal expansion (CTE) has a direct impact on spring-in. A tool with a CTE of 25 μm/m/°C gave significantly more spring-in than a tool with zero CTE.

1.3. Outline and objective

The effect of several parameters on spring-in have been reported in the literature [1–12], as discussed above. However, because of the large number of parameters that vary between studies, it is difficult to draw any general conclusions from this body of work. This paper presents a large amount of experimental data that examines the effect of design and process parameters on spring-in and warpage of composite angles with a symmetrical lay-up. The objective is to determine the effect several design and process parameters have on spring-in, and how the different parameters interact. The paper examines the individual and interactive effects of five design parameters: part shape, lay-up, flange length, part thickness, and part angle, and three process parameters: tool material, tool surface, and cure cycle, on spring-in and warpage of angled composite laminates. The parameters studied were selected based on previous research by the authors [10]. The presented results are based on six sets of experiments, which are fully described in the Appendix. However, only select results are presented in the main text for ease of interpretation. The first experiment was an eight-factor fractional factorial designed experiment. This design allows the examination of eight parameters simultaneously to identify key parameters. The following five experiments were performed to focus on select parameters and to examine interactive effects in more detail.

2. Calculation of anisotropy spring-in components

Eq. (1) was used to calculate approximate values of the anisotropy spring-in component for parts manufactured in the current study. The parameters used in the calculations and the predicted spring-in angles are shown in Table 1. The material used for all parts in this study was the T-800H/3900–2 carbon/epoxy unidirectional prepreg, which is a non-bleed, toughened system manufactured by the Toray Company. There are several papers in the literature with slightly different elastic and thermo-elastic properties for this material. The properties used in the present analysis are in close agreement to those presented in Ref. [23]. The thermal component of the spring-in angle $\Delta\theta_{CTE}$, i.e. the first term in Eq. (1), develops during cool-down, when the material is fully cured. $\Delta\theta_{CTE}$ represents a lower bound for the total anisotropy spring-in component as any cure shrinkage would add to this value. The coefficients of thermal expansion used to evaluate $\Delta\theta_{CTE}$ are those at 100 °C, the average of cure and room temperatures. The longitudinal coefficient of thermal expansion, α_l, for the quasi-isotropic laminate was calculated from the lamina properties using laminate plate theory. The transverse coefficient of thermal expansion, α_t, for the quasi-isotropic laminate was calculated from the lamina properties using the methods developed in Ref. [19], assuming plane stress through the thickness of the laminate.

Table 1
Anisotropy component calculations—parameters and results

Parameters	$[0]_n$		$[0/45/-45/90]_{ns}$	
α_l (m/m/°C)	-2.55×10^{-8}		2.53×10^{-6}	
α_t (m/m/°C)	4.05×10^{-5}		5.95×10^{-5}	
ϕ_l (m/m)	8.05×10^{-5}		2.91×10^{-4}	
ϕ_t (m/m)	3.76×10^{-3}		5.43×10^{-3}	
Cure temperature (°C)	180		180	
Room temperature (°C)	20		20	
Initial angle, θ (°)	90	45	90	45
$\Delta\theta$ (°)	0.58	0.29	0.82	0.41
$\Delta\theta_{CS}$ (°)	0.32	0.16	0.46	0.23
$\Delta\theta = \Delta\theta_{CTE} + \Delta\theta_{CS}$ (°)	0.90	0.45	1.28	0.64

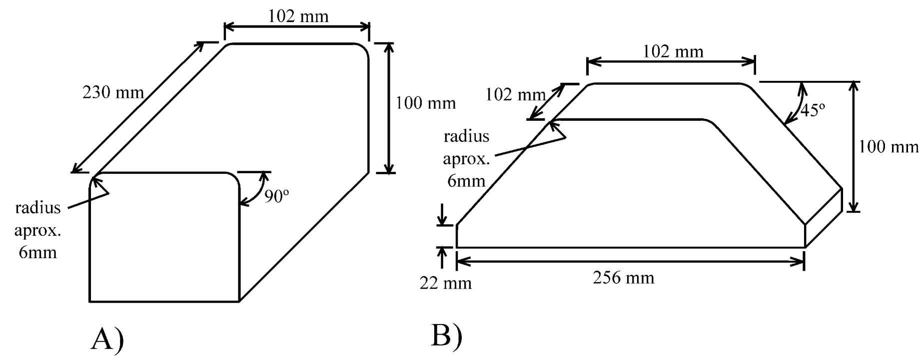

Fig. 2. Geometry of the tools used in this study: (a) 90° tool, (b) 45° tool.

The cure shrinkage anisotropy component, $\Delta\theta_{CS}$, i.e. the second term in Eq. (1), develops while the resin is curing. The evaluation of $\Delta\theta_{CS}$ is not as straightforward as for $\Delta\theta_{CTE}$ because it is dependent on the resin cure history. The amount of cure shrinkage causing residual stress build-up is not known for this material, but typical total volumetric cure shrinkage (V_{sh}^{T}) values quoted in the literature for epoxy resins range between 1 and 10% [20–22], depending on how measurements are performed and the type of resin used. Higher values are obtained if the shrinkage is measured right from the beginning of polymerization than if shrinkage is only measured when the resin is solid and has developed appreciable stiffness. Values for ϕ_l and ϕ_t were estimated for a unidirectional laminate by using a simple rule of mixtures, with the assumption that a resin volumetric shrinkage (V_{sh}) of 2% contributes to spring-in. The value of 2% is a rough estimate based on the assumption that the total volumetric shrinkage is 10%, of which 60% occurs prior to gelation, and of the remaining 40%, only half occurs after the resin has developed significant modulus. This assumption gives the result that the cure shrinkage contribution is approximately half that of the thermal component, which can be considered an upper bound. Note that the predictions of spring-in will only be used in a qualitative sense in this study. The ranges of ϕ_l and ϕ_t for the quasi-isotropic parts were calculated using the same methods as for calculation of α_l and α_t. Values of $\Delta\theta_{CS}$ and $\Delta\theta$ were then calculated from these parameters for each lay-up using Eq. (1).

3. Experimental

3.1. Tool and part geometries

This section describes the overall range of part and tool geometries used in this study. A more detailed description of each part is found in the Appendix. The tool geometries used in this study are shown in Fig. 2. The tools consist of solid blocks of 6061-T6 aluminum or A36 steel. The tools were machined to an angle of either 90° or 45°, with a corner radius of approximately 6 mm. The tool surface was in a smooth "as-milled" condition. The parts made were either unidirectional laminates $[0]_n$ or quasi-isotropic laminates $[0,+45,-45,90]_{ns}$. The parts were C or L-shaped with flange lengths of either 57 mm or 89 mm, and a thickness of either 8 or 16 plies, i.e. 1.6 mm and 3.2 mm respectively (Fig. 3). The width of all parts was 50 mm and the web length of the C-shaped parts was 102 mm.

3.2. Lay-up and processing

The tool surfaces were cleaned with acetone to remove traces of oil and dirt between lay-ups. Two or three coats of release agent (Multishield) were then applied over the entire surface, allowing each coat to air-dry for 15 min before application of the next coat. A fluorinated ethylene propylene (FEP) sheet was placed over the release agent before the prepreg was laid up on the tool for some parts (see Appendix). A vacuum of approximately −1 atmosphere (−30 in Hg) was applied for 15 min every four plies to consolidate the part and remove entrapped air. Thermocouples were placed on the parts, near the tool surface and near the bag surface. The parts were then covered with a non-permeable FEP sheet and a breather fabric and placed inside a vacuum bag. No edge dams were used. Once the lay-up was complete, the assemblies (tools, parts, and vacuum

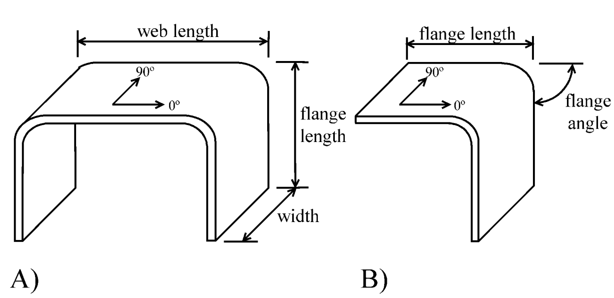

Fig. 3. Part geometries: (a) C-shaped part, (b) L-shaped part.

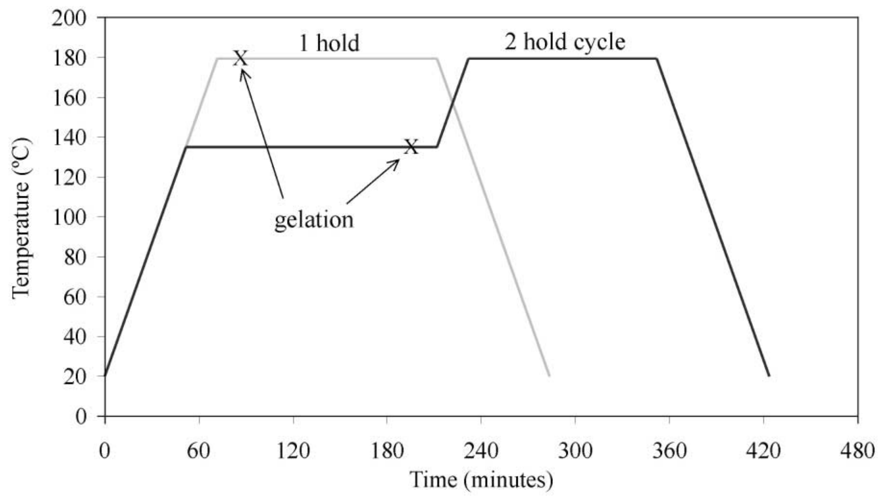

Fig. 4. Schematic of the used cure cycles. The approximate point of gelation was calculated based on cure kinetics equations for the material.

bags) were placed inside an autoclave and cured at a relative pressure of 5.8 atmospheres (85 psi). Two different cure cycles were used: a one-hold and a two-hold cycle (Fig. 4). The one-hold cure cycle was designed so that gelation of the resin occurs during the temperature hold. The two-hold cycle was designed to achieve gelation prior to the second heat-up. The point of gelation was estimated based on calculations using cure kinetics equations for the prepreg system. After processing, the parts were left to cool down to room temperature before they were debagged and removed from the process tool.

3.3. Measurements

Tool angles were measured with a Mitutoyo Pro 3600 digital protractor, with a measurement resolution of 0.01° for the 90° tools, and a resolution of 0.1° for the 45° tools. Five measurements were taken and the measurements were repeatable to within $\pm 0.02°$.

After debagging, approximately 1 cm was trimmed off the width (Fig. 3) of each part using an IMER Combi 250/500 diamond saw to eliminate the effect of edge thinning on spring-in measurements. The ends were not trimmed but measurements were not taken closer than approximately 5 mm from the ends to avoid edge effects. The surfaces were polished on metallographic polishing wheels with a 600 grit paper. Fig. 5 shows photographs of representative C and L-shaped parts manufactured in the study. A Hewlett Packard ScanJet 4c scanner was used to create three images of each cross section at a resolution of 600 dpi. The angles were measured using digital image analysis (Fig. 6). Spring-in was calculated as the difference between corresponding part and tool angles. Variability in part angle measurement is addressed in the Appendix.

4. Results

The measured spring-in of the parts made in experiment 1 is shown in Fig. 7 together with the predicted spring-in, $\Delta\theta$, using Eq. 1 (Table 1). Although the predicted spring-in is approximate due to uncertainty in the cure shrinkage component, the figure shows that spring-in varies significantly with design and process parameters and that there appear to be mechanisms in addition to anisotropy of cure shrinkage and thermal expansion that contribute to spring-in. For detailed information about each of the parts in Fig. 7, see Table A1. A closer examination of the effect of individual design and process parameters will now be made.

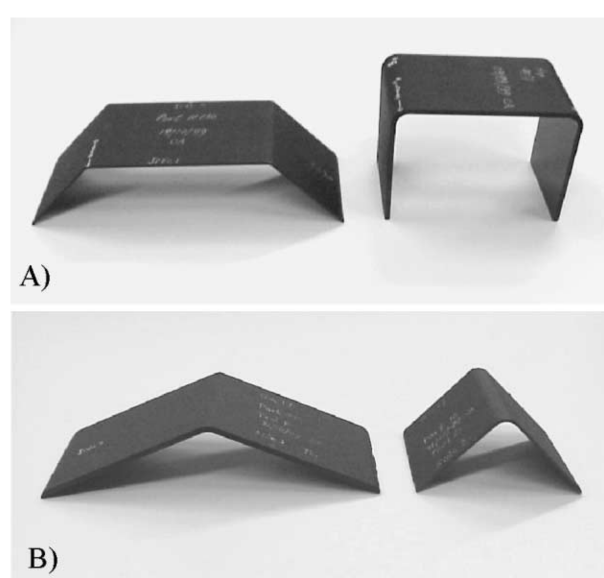

Fig. 5. Photographs of composite parts prepared in this study: (a) C-shaped parts, (b) L-shaped parts.

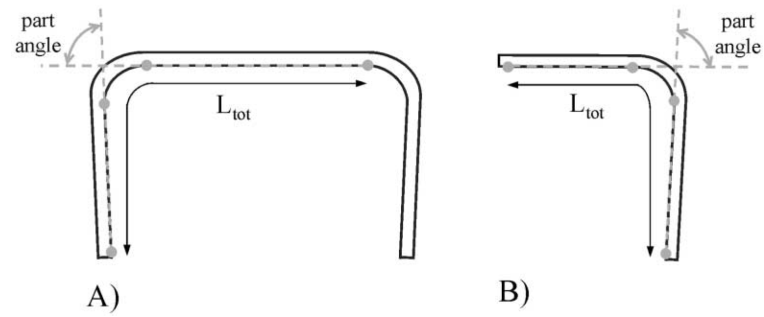

Fig. 6. Schematic of how part angle measurements were performed on (a) C-shaped parts, and on (b) L-shaped parts. Straight lines were fitted to two points on each flange or web segment.

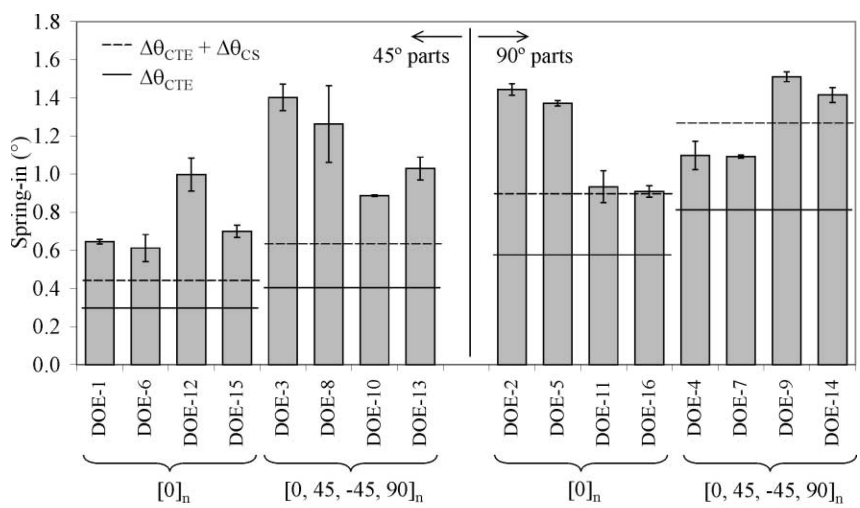

Fig. 7. Measured spring-in from experiment 1. Solid and dashed lines represent spring-in predictions using Eq. (1). Parts are described in Table A1.

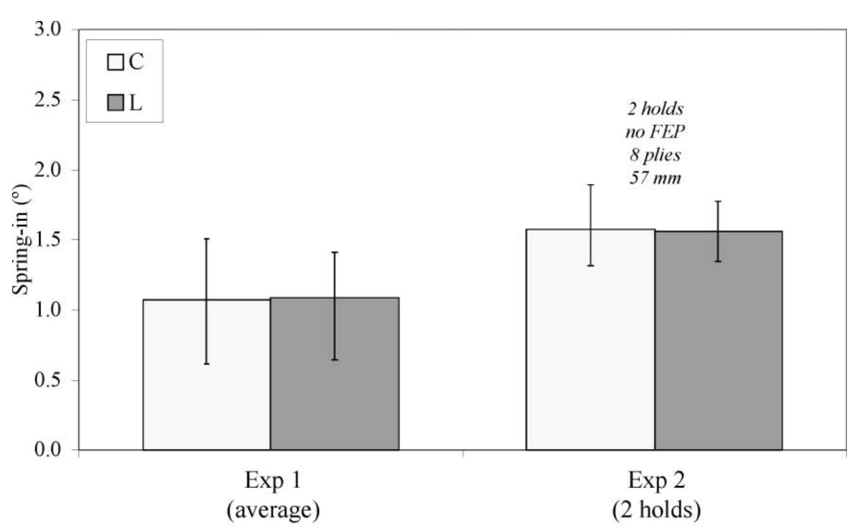

Fig. 8. Effect of part shape on spring-in. The ranges shown represent the maximum and minimum measured values for each data set. Parts are described in Tables A1 and A2.

4.1. Effect of intrinsic parameters

Fig. 8 shows the effect of part shape on spring-in, based on data from experiments 1 and 2. The figure shows that part shape has little effect on spring-in in the present study, which disagrees with previous work [10] where C-shaped parts exhibited greater spring-in than L-shaped parts by about 30%. The reason for this disagreement is not known, but it could be related to differences in design and process conditions.

Fig. 9 shows the effect of part lay-up on spring-in, based on data from experiments 1, 4, and 5. The figure shows that quasi-isotropic parts have greater spring-in than unidirectional 0° parts. This result is in agreement with the anisotropy calculations of spring-in (Table 1), which show that anisotropy-driven spring-in is greater for quasi-isotropic than for unidirectional parts. The physical reason for this is that the through-thickness contraction is greater for quasi-isotropic laminates than for unidirectional ones because of Poisson's effects [19]. The findings agrees with results from the literature [3,6,10].

Fig. 10 shows the effect of part thickness on spring-in based on data from experiments 1, 3 and 4. It is shown that thin parts have greater spring-in than corresponding thick parts, especially when no FEP release ply is used in a two-hold cure cycle (experiments 3 and 4). Note that the parts prepared in experiment 4 have longer flanges than those prepared in experiment 3,

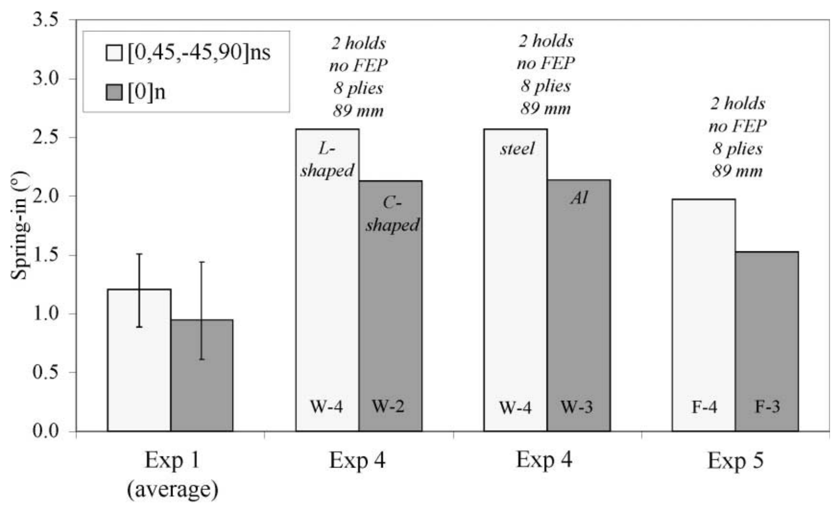

Fig. 9. Effect of part lay-up on spring-in. The ranges shown represent the maximum and minimum measured values for each data set. Parts are described in Tables A1, A4, and A5.

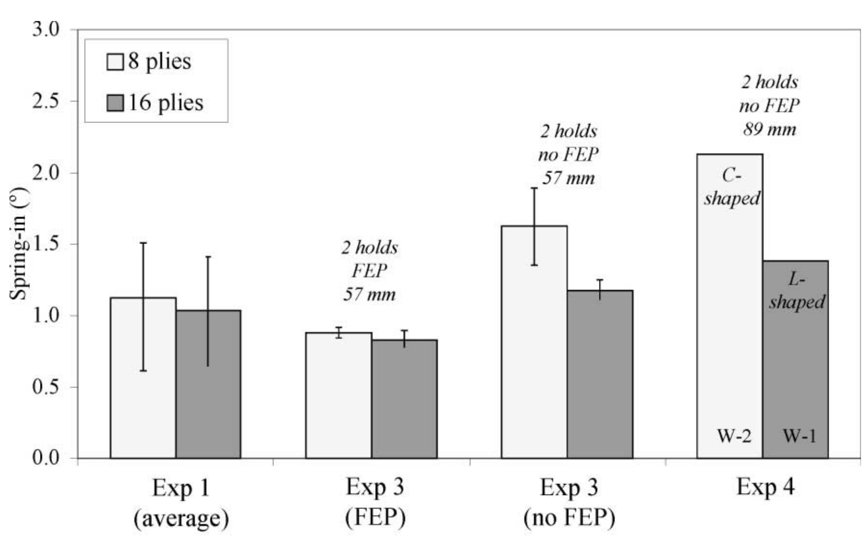

Fig. 10. Effect of part thickness on spring-in. The ranges shown represent the maximum and minimum measured values for each data set. Parts are described in Tables A1, A3, and A4.

suggesting that the effect of part thickness increases with increasing flange length.

To compare the effect of flange or part length between L and C-shaped parts, the total length of the "flanges", or flat sections, corresponding to a given corner (L_{tot}), must be defined and determined. For an L-shaped part, L_{tot} is equal to twice the flange length (L_{flange}), while for a C-shaped part, L_{tot} is equal to the sum of the web length (L_{web}) and the flange length. This definition is based on how the spring-in angles are measured (Fig. 6). Fig. 11 shows the effect of part length on measured spring-in, based on parts from experiments 1, 2, 3, and 4. The figure shows that spring-in increases with increasing part length, L_{tot}, and that the effect of part length is greater for 8-ply parts than for 16-ply parts.

4.2. Effect of extrinsic parameters

Fig. 12 shows the effect of cure cycle on the measured spring-in, based on data from experiments 1, 2, 5, and 6. The figure shows that parts processed using a two-hold cycle have substantially more spring-in than parts processed using a single hold cycle. For a schematic of the cure cycles used, see Fig. 4. These findings are in agreement with Refs. [10,11] but are in disagreement with Ref. [13].

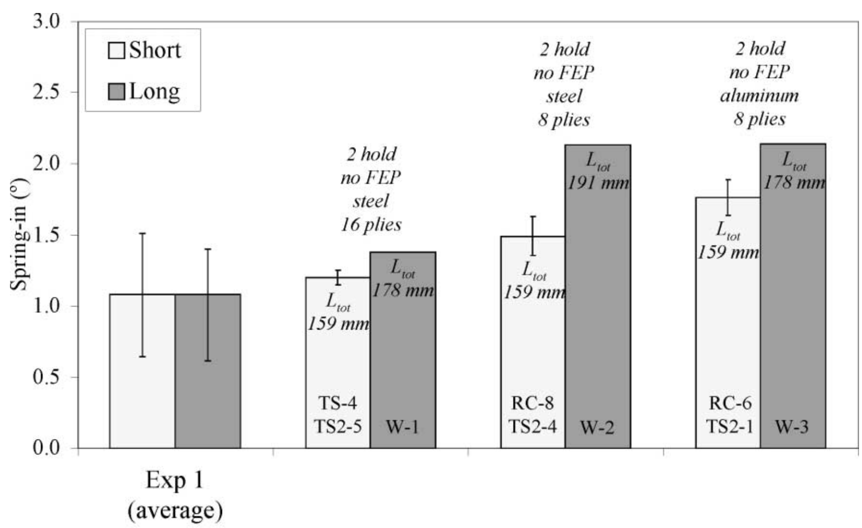

Fig. 11. Effect of part length on spring-in. The ranges shown represent the maximum and minimum measured values for each data set. Parts are described in Tables A1–A4.

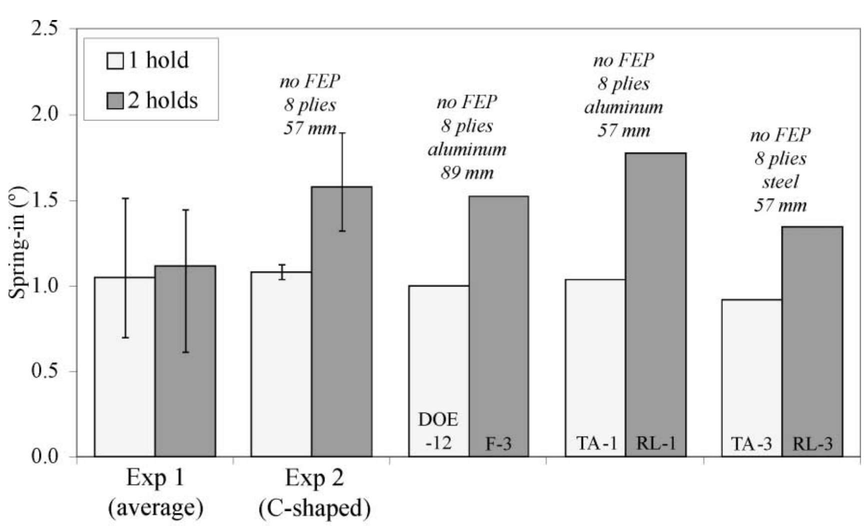

Fig. 12. Effect of cure cycle on spring-in. The ranges shown represent the maximum and minimum measured values for each data set. Parts are described in Tables A1–A3, and A6.

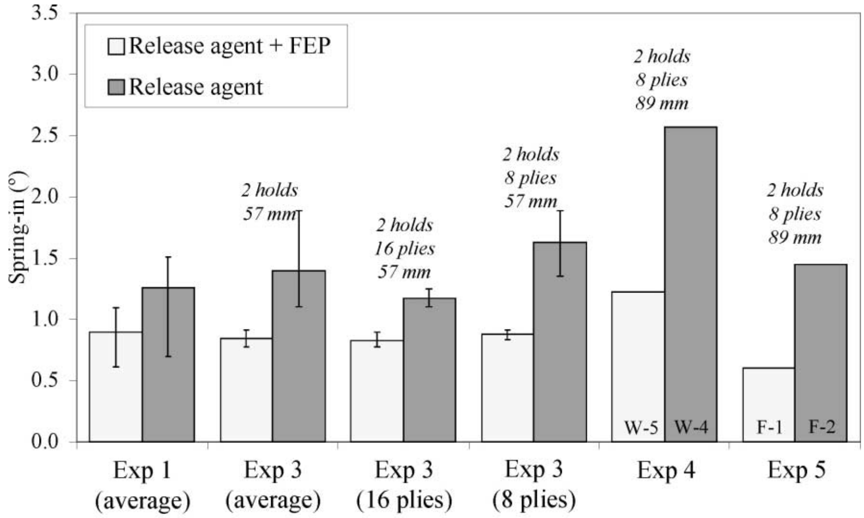

Fig. 13. Effect of tool surface on spring-in. The ranges shown represent the maximum and minimum measured values for each data set. Parts are described in Tables A1 and A3–A5.

Fig. 13 shows the effect of the tool surface condition (release agent or release agent + FEP release film) on the measured spring-in, based on data from experiments 1, 3, 4 and 5. As shown in the figure, the effect of tool surface condition is substantial. Parts processed without an FEP release sheet have considerably greater spring-in than those processed with an FEP sheet. Note that in both cases, the parts came readily off the tool after processing, and no "sticking" was observed. Fig. 13 shows that the greatest difference between parts processed with and without an FEP film is for long, thin parts (experiment 4).

Fig. 14 shows the effect of tool material on measured spring-in, based on data from experiments 1, 2, 3, 4, and 6. The figure shows that aluminum tooling always gives more spring-in than steel tooling but that the difference is only significant in certain cases. There are clearly other parameters that interact with the tooling material in affecting spring-in. A closer look at the data reveals that the tool material has little effect on spring-in for parts processed with a 1-hold cure cycle, but beyond that it is difficult to draw any clear conclusions from the data.

4.3. Effect of measurement technique

The measured spring-in angles presented up to now are based on measurements of two points on each side

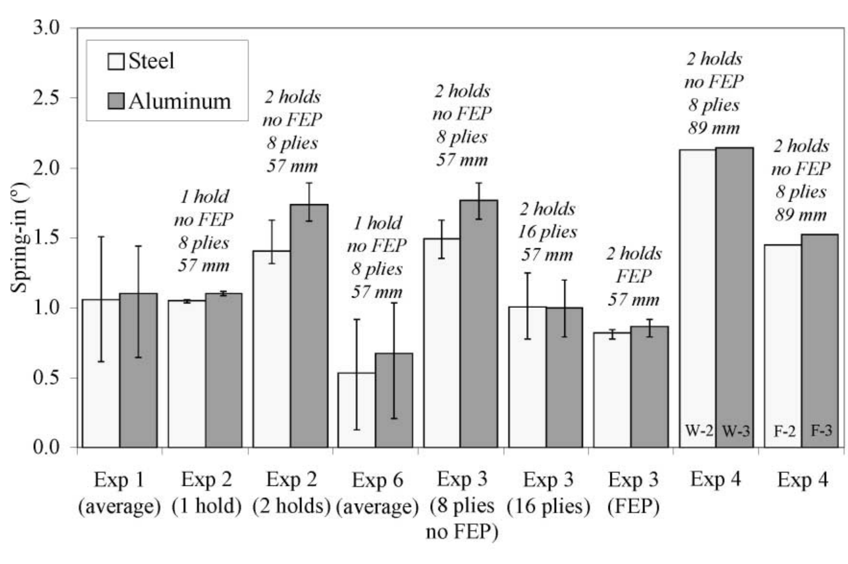

Fig. 14. Effect of tool material on spring-in. The ranges shown represent the maximum and minimum measured values for each data set. Parts are described in Tables A1–A4, and A6.

of a corner (Fig. 6). The reason why this measurement technique is used is that it is relatively straightforward, and that process-induced deformations of angled composite laminates are typically quantified in terms of a spring-in angle in industry. However, although the only process-induced deformation directly observable with the naked eye for the parts made in this study is spring-in, careful observation showed that the flat sections of all parts warped away from the tool. To quantify this warpage, the curvature of every flange and web were measured using digital image analysis. The locations of 13 points along each flange or web on the tool side of the part were recorded and the measured profiles were plotted as shown in Fig. 15. While the warpage was not directly observable with the naked eye, it was in many cases great enough to significantly increase the measured spring-in.

For a part without flange or web warpage, the spring-in measured at the corner is the same as that measured anywhere along the web/flanges. When warpage is present, however, spring-in results will be affected by the measurement locations. When analysing spring-in it is thus important to consider where and how the measurements are taken. In the presence of warpage, the total spring-in ($\Delta\theta_{\text{total}}$) can be separated into two components: a corner component ($\Delta\theta_{\text{corner}}$) and a flange/web warpage component ($\Delta\theta_{\text{warpage}}$), see Eqs. (2a) and (2b), and Fig. 16.

$$\Delta\theta_{\text{total}} = \Delta\theta_{\text{corner}} + \Delta\theta_{\text{warpage}} \tag{2a}$$

$$\Delta\theta_{\text{total}} = \Delta\theta_{\text{corner}} + \left(\Delta\theta_{\text{flange A warpage}} + \Delta\theta_{\text{flange B warpage}}\right) \tag{2b}$$

The effect of warpage on spring-in was measured as the angle formed by the tangent to the flange or web profile on the side adjacent to the corner, and a line drawn between the two extremities of the flange or web (A–A′), see Fig. 16. Although the maximum deflection of the flange of the part shown in Fig. 15 is only 0.2 mm for a flange that is 89 mm long, this warpage increases the measured spring-in by approximately 0.48°. This shows how sensitive the spring-in measurement technique is to flange and web warpage. The total $\Delta\theta_{\text{warpage}}$ for a given angle is the sum of the warpage component for each flange, i.e. $\Delta\theta_{\text{flange A warpage}}$ and $\Delta\theta_{\text{flange B warpage}}$ [Eq. (2b) and Fig. 16]. The true corner spring-in can be calculated by subtracting the measured $\Delta\theta_{\text{warpage}}$ from the total measured spring-in. The corner component, the warpage component, and the total spring-in for the parts made in experiments 1–6 are presented in Tables A1–A6. Note that by defining $\Delta\theta_{\text{warpage}}$ in this way, $\Delta\theta_{\text{warpage}}$ will increase with increasing distance between the measurement points used.

Fig. 17 shows the spring-in components for the parts made in experiment 1 together with the predicted (corner) spring-in using Eq. (1). The figure shows that the large variation in the total spring-in is largely due to variations in the warpage component, and that the corner component is relatively constant and in reasonable agreement with the predictions of Eq. (1). The process and design parameters that have the greatest effect on warpage will now be presented.

Fig. 18 shows the effect of laminate thickness on spring-in due to warpage. It is interesting to note that it is flange and web warpage that give rise to the large measured total spring-in seen in Fig. 10 for the 8-ply parts processed without a FEP release film.

Fig. 19 shows the effect of part length on spring-in due to warpage. The figure shows that warpage has a larger effect on the measured spring-in for longer parts than for shorter ones, and that the effect is especially significant for thin parts. Note that the longer parts had a greater distance between the measurement points (Fig. 6) which by itself will give a larger spring-in due to warpage.

Fig. 20 shows the effect of cure cycle on spring-in due to warpage. The figure shows that warpage is sub-

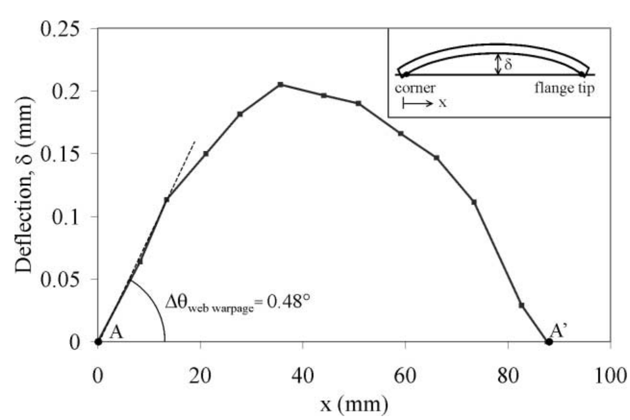

Fig. 15. Process-induced curvature of the web of part TS2–4 (Table A3).

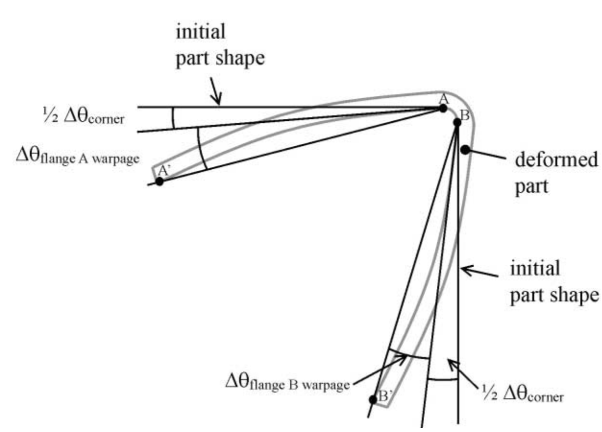

Fig. 16. Definition of spring-in components.

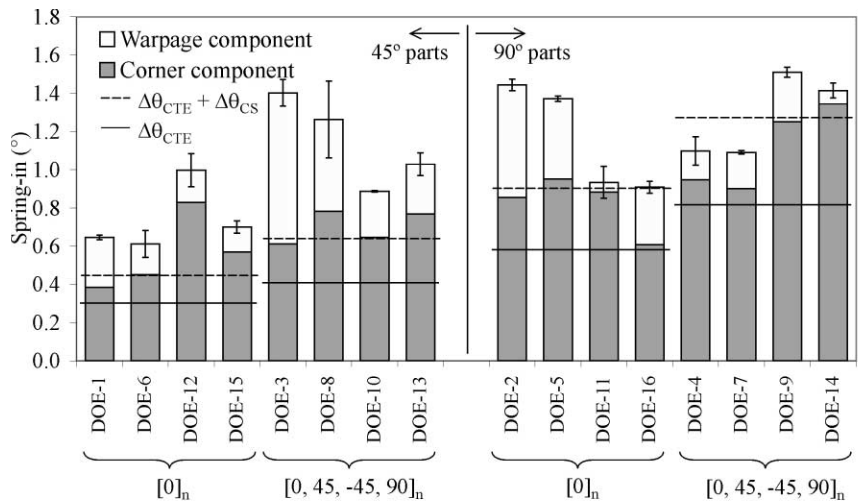

Fig. 17. Measured spring-in components from experiment 1. The range shown represents 1/2 (maximum measured value - minimum measured value) for each part. Solid and dashed lines represent spring-in predictions using Eq. (1).

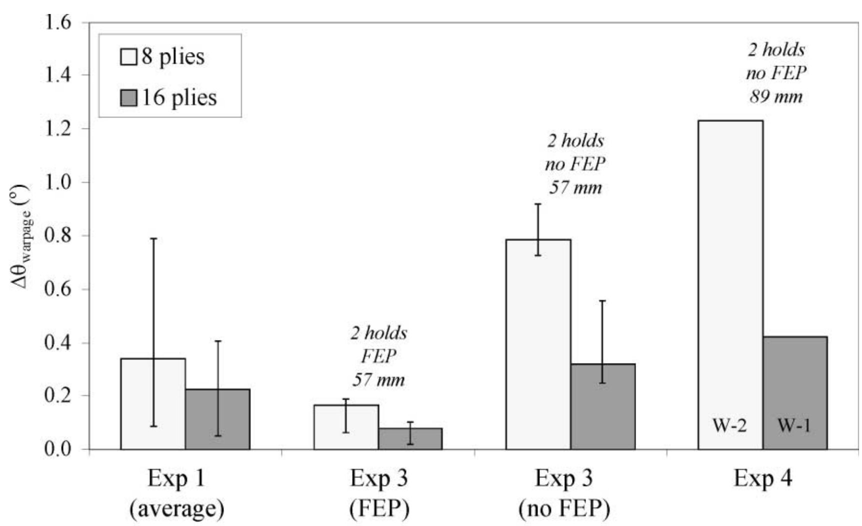

Fig. 18. Effect of part thickness on warpage. The ranges shown represent the maximum and minimum values for each data set. Parts are described in Tables A1, A3, and A4.

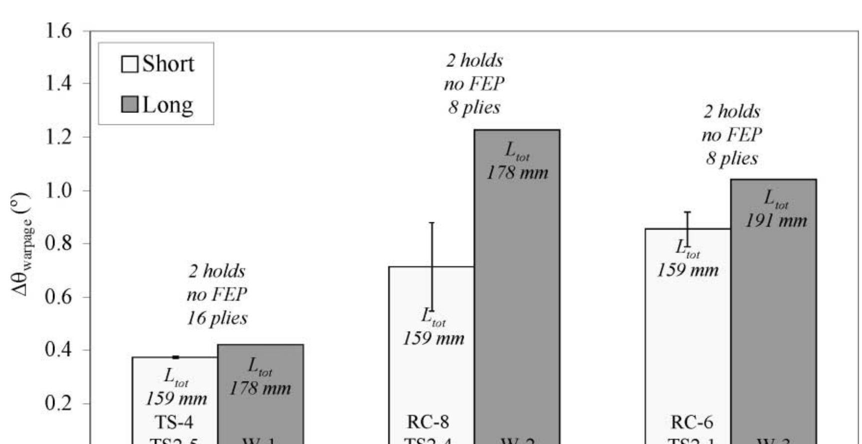

Fig. 19. Effect of part length on warpage. The ranges shown represent the maximum and minimum measured values for each data set. Parts are described in Tables A1–A4.

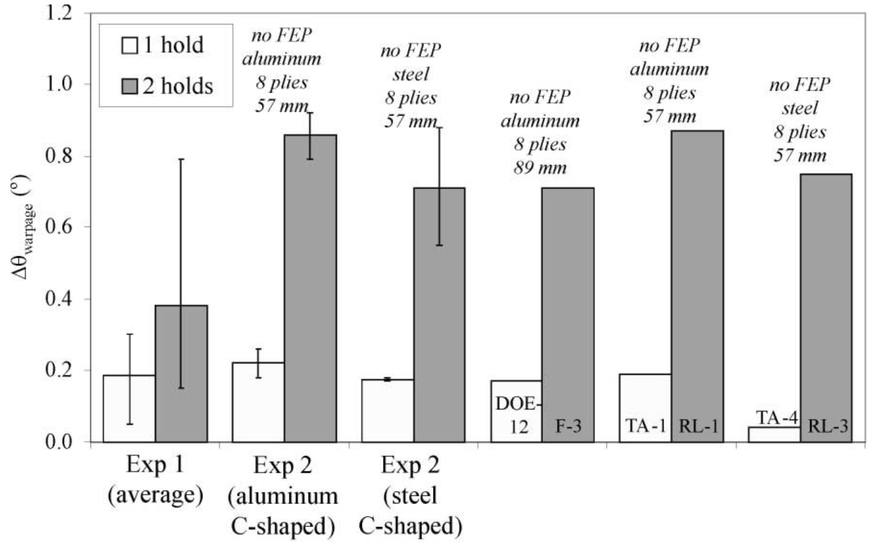

Fig. 20. Effect of cure cycle on warpage. The ranges shown represent the maximum and minimum measured values for each data set. Parts are described in Tables A1–A3, and A6.

stantially greater for parts processed with a two-hold cycle than for parts processed with a one-hold cycle. The cure cycles are shown in Fig. 4.

Fig. 21 shows the effect of using a FEP release sheet on spring-in due to warpage. The figure shows that spring-in due to warpage is significantly reduced when a FEP release sheet is used.

5. Discussion

Many of the findings in this study are in agreement with previously published work but some are not. For example, the effect of cure cycle found in this study is in agreement with previous work by the authors [10,11] but in disagreement with other published work [13]. The different trends observed are likely caused by different mechanisms, which are dominant at different process conditions.

Warpage of flat sections was found to be of significance in this study. The results indicate that warpage is caused by mechanical shear interaction between the tool and part at the tool–part interface, which is a phenomenon studied earlier [14–18]. However, warpage is likely to be dependent on the slenderness (length to thickness) ratio of the laminate and may be of little significance for thicker and shorter laminates [16]. The results also indicate that much of the variability in spring-in is due to warpage, so that by controlling warpage more uniform parts can be made.

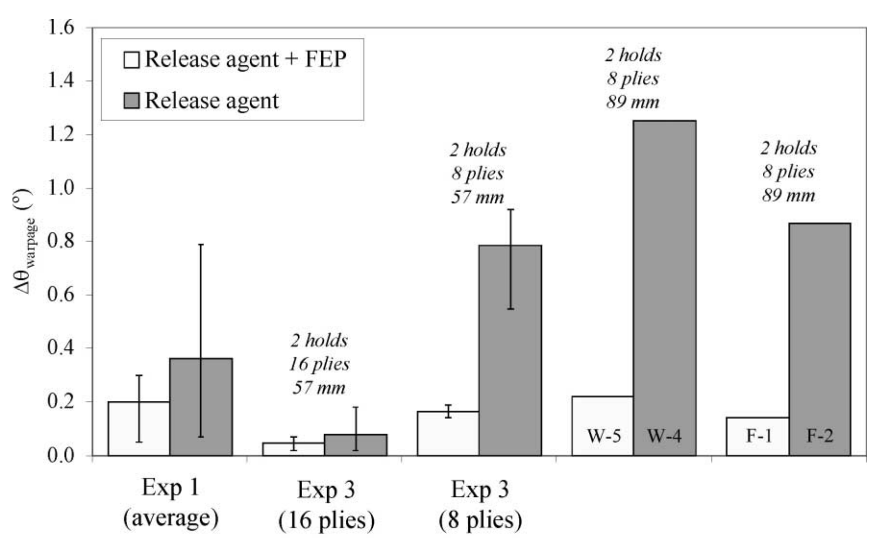

Fig. 21. Effect of tool surface on warpage. The ranges shown represent the maximum and minimum measured values for each data set. Parts are described in Tables A1 and A3–A5.

Although this study sheds some light on parameters affecting spring-in and warpage of angled composite laminates and demonstrates the importance of how spring-in angles are defined and measured, the conclusions drawn should be used with caution outside the parameter range of this study. Despite an increasing understanding of the fundamental mechanisms that drives process induced deformation of composite laminates, the fundamental understanding required to reliably scale the observations from one set of conditions to vastly different conditions is still under development.

6. Conclusions

The objective of this work was to determine the effect of design and process parameters on spring-in of angled thermoset laminates. The main conclusions from the current work are as follows:

- Spring-in varies greatly as a function of design and process parameters for the parts made in the current study.
- For practical reasons, spring-in is usually measured based on the deflection of the flanges away from the corner. The current work showed that spring-in measured this way is sensitive to flange/web warpage. Even when the warpage is too small to be perceived with the naked eye, it can significantly contribute to the measured spring-in.
- A measurement method was developed to separate spring-in into two distinct components: a corner component and a flange/web warpage component.
- The corner component of spring-in was shown to be primarily the product of thermal and cure shrinkage. This component was found to be repeatable for a given part design and cure temperature, and can be predicted using a simple equation [Eq. (1)]. For a given material and cure temperature, parameters affecting the corner component are the initial part angle and the part lay-up.
- The warpage component of spring-in was found to be strongly dependent on the process conditions. A number of parameters were found to affect the warpage component, including the laminate thickness and flange length, as well as the cure cycle, the tool material, and the tool surface condition. While the laminate thickness and flange length are inherent elements of a part design and cannot be modified during processing, the process conditions can be altered to minimize this component of the total spring-in.
- Table 2 summarizes the general importance of each of the studied parameters on the total spring-in, and indicates which component of spring-in (i.e. corner or warpage) is affected by each parameter.

Based on the results of this study, three simple rules to minimize the variability of spring-in in production are proposed:

1. Control the cure cycle to avoid early gelation. Ensure that all parts gel at the final hold temperature.
2. Select tooling material that as closely as possible matches the coefficient of thermal expansion of the part.
3. Use a fluorinated ethylene propylene sheet, or other release ply, in addition to release agent at the tool-part interface. This is especially important when processing long and thin parts.

Table 2
Summary of the importance of the studied design and process parameters on spring-in, and weather they affect spring-in or warpage

Parameter	Importance[a]	Affects spring-in	Affects warpage	Type
Tool surface (FEP/Release agent)	High		X	Extrinsic
Thickness (8/16 plies)	High		X	Intrinsic
Part length (~114–191 mm)	High		X	Intrinsic
Cure cycle (1/2-hold)	High		X	Extrinsic
Lay-up ([0]*n*/[0,45,−45,90]*ns*)	Medium	X	?[b]	Intrinsic
Part angle (90°/45°)	Medium	X	?[b]	Intrinsic
Tool material (aluminum/steel)	Medium		X	Extrinsic
Part shape (C/L)	Low			Intrinsic

[a] Indication of the impact of the parameter on the total spring-in. Parameters with a maximum effect of less than 0.20° are here classified as of "Low" importance, those with a maximum effect between 0.20° and 0.50° are classified as of "Medium" importance, and those with a maximum effect greater than 0.50° are classified as of "High" importance.

[b] Question mark indicates that the effect is not clear based on the data available.

Acknowledgements

The authors would like to thank Dr. Karl Nelson and Mr. Kurtis Willden of The Boeing Company in Seattle for providing materials, Mr. Roger Bennett and Mr. Ross McLeod of The Department of Metals and Materials Engineering at UBC for their technical support, and the Natural Sciences and Engineering Research Council of Canada for financial support of the research. Finally we would like to thank past and current members of the UBC Composites group, in particular Dr. Anoush Poursartip, for significant interaction and for increasing our understanding of processing of composite materials.

Appendix

Experimental results

In experiment 1, eight parameters were investigated in a fractional factorial experiment (Table A1). The high and low settings for each parameter were selected to reflect typical process conditions. A 28–4 resolution IV experiment [25] was used, allowing the examination of the effect of eight parameters simultaneously in a significantly reduced number of experiments. Each parameter was varied between two values. In experiment 2, a total of 12 parts were prepared to examine the effect of part shape, tool material, cure cycle and a rubber caul sheet. The parts are described in Table A2. Experiment 3 consists of 12 parts examining the effect of part thickness, tool material and tool surface on spring-in. These parts are described in Table A3. Experiments 4 and 5 were designed to examine the effect of flange length for parts with initial angles of 90° and 45°, respectively. These two experiments also provide additional information about the effect of part thickness, part angle, lay-up, tool surface, and tool material. A description of the parts prepared for experiments 4 and 5 is given in Tables A4 and A5. Six parts were prepared in experiment 6 to examine the effect of tool angle and tool material on spring-in (Table A6).

Measurement variability

Each part was measured a minimum of three times using a minimum of two scanned images, taken at different locations on the PC scanner. The measurement variability is shown for each part in terms of a range between the minimum and the maximum measurement, i.e. (max−min)/2. The measured ranges, shown in Tables A1–A6 are well below ±0.1° for almost all parts. Part DOE-8 (Table A1), however, had a measurement variability of ±0.20°. Closer examination showed that the spring-in of the two flanges of part DOE-8 differed

Table A1
Experiment 1: design and results

Part ID	Factor								$\Delta\theta_{total}$ (°)	Range[b] (°)	$\Delta\theta_{corner}$ (°)	$\Delta\theta_{warpage}$ (°)
	1	2	3	4	5	6	7	8				
	Part shape	Lay-up	Flange length (mm)	Thickness (plies)	Part angle (°)	Tool material	Tool surface[a]	Cure cycle (holds)				
DOE-1	L	$[0]_{16}$	57	16	45	Aluminum	Release agent (2) + FEP	2	0.65	±0.01	0.39	0.26
DOE-2	C	$[0]_8$	57	8	90	Aluminum	Release agent (2)	2	1.44	±0.03	0.85	0.59
DOE-3	L	$[0,45,-45,90]_s$	57	8	45	Steel	Release agent (2)	2	1.40	±0.07	0.61	0.79
DOE-4	C	$[0,45,-45,90]_{2s}$	57	16	90	Steel	Release agent (2) + FEP	2	1.10	±0.07	0.95	0.15
DOE-5	L	$[0]_{16}$	89	16	90	Steel	Release agent (2)	2	1.37	±0.01	0.95	0.42
DOE-6	C	$[0]_8$	89	8	45	Steel	Release agent (2) + FEP	2	0.61	±0.07	0.45	0.16
DOE-7	L	$[0,45,-45,90]_s$	89	8	90	Aluminum	Release agent (2) + FEP	2	1.09	±0.01	0.90	0.19
DOE-8	C	$[0,45,-45,90]_{2s}$	89	16	45	Aluminum	Release agent (2)	2	1.26	±0.20	0.78	0.48
DOE-9	C	$[0,45,-45,90]_s$	89	8	90	Steel	Release agent (2)	1	1.51	±0.03	1.25	0.26
DOE-10	L	$[0,45,-45,90]_{2s}$	89	16	45	Steel	Release agent (2) + FEP	1	0.89	±0.00	0.65	0.24
DOE-11	C	$[0]_{16}$	89	16	90	Aluminum	Release agent (2) + FEP	1	0.94	±0.08	0.89	0.05
DOE-12	L	$[0]_8$	89	8	45	Aluminum	Release agent (2)	1	1.00	±0.09	0.83	0.17
DOE-13	C	$[0,45,-45,90]_s$	57	8	45	Aluminum	Release agent (2) + FEP	1	1.03	±0.06	0.77	0.26
DOE-14	L	$[0,45,-45,90]_{2s}$	57	16	90	Aluminum	Release agent (2)	1	1.41	±0.04	1.34	0.07
DOE-15	C	$[0]_{16}$	57	16	45	Steel	Release agent (2)	1	0.70	±0.03	0.57	0.13
DOE-16	L	$_8$	57	8	90	Steel	Release agent (2) + FEP	1	0.91	±0.03	0.61	0.30
							Average		1.08			

[a] The number within parenthesis denotes the number of coats of release agent applied. FEP denotes the use of a fluorinated ethylene propylene sheet.

[b] The range shown represents 1/2 (maximum measured value—minimum measured value).

Table A2
Experiment 2: design and results

Part ID	Part shape	Lay-up	Flange length (mm)	Thickness (plies)	Part angle (°)	Tool material	Tool surface[a]	Cure cycle (holds)	Rubber caul	$\Delta\theta_{total}$ (°)	Range[b] (°)	$\Delta\theta_{corner}$ (°)	$\Delta\theta_{warpage}$ (°)
RC-1	C	$[0]_8$	57	8	90	Aluminum	Release agent (3)	1	Yes	1.09	±0.01	0.83	0.26
RC-2	C	$[0]_8$	57	8	90	Aluminum	Release agent (3)	1	No	1.12	±0.02	0.94	0.18
RC-3	C	$[0]_8$	57	8	90	Steel	Release agent (3)	1	Yes	1.06	±0.01	0.89	0.17
RC-4	C	$[0]_8$	57	8	90	Steel	Release agent (3)	1	No	1.04	±0.05	0.86	0.18
RC-5	C	$[0]_8$	57	8	90	Aluminum	Release agent (3)	2	Yes	1.62	±0.02	0.75	0.87
RC-6	C	$[0]_8$	57	8	90	Aluminum	Release agent (3)	2	No	1.89	±0.03	0.97	0.92
RC-7	C	$[0]_8$	57	8	90	Steel	Release agent (3)	2	Yes	1.32	±0.04	0.62	0.70
RC-8	C	$[0]_8$	57	8	90	Steel	Release agent (3)	2	No	1.36	±0.02	0.81	0.55
RL-1	L	$[0]_8$	57	8	90	Aluminum	Release agent (3)	2	Yes	1.78	±0.02	0.91	0.87
RL-2	L	$[0]_8$	57	8	90	Aluminum	Release agent (3)	2	No	1.76	±0.03	0.96	0.80
RL-3	L	$[0]_8$	57	8	90	Steel	Release agent (3)	2	Yes	1.34	±0.04	0.59	0.75
RL-4	L	$[0]_8$	57	8	90	Steel	Release agent (3)	2	No	1.37	±0.05	0.74	0.63

[a] The number within parenthesis denotes the number of coats of release agent applied.
[b] The range shown represents 1/2 (maximum measured value—minimum measured value).

Table A3
Experiment 3: design and results

Part ID	Part shape	Lay-up	Flange length (mm)	Thickness (plies)	Part angle (°)	Tool material	Tool surface[a]	Cure cycle (holds)	$\Delta\theta_{total}$ (°)	Range[b] (°)	$\Delta\theta_{corner}$ (°)	$\Delta\theta_{warpage}$ (°)
TS2–1	C	$[0]_8$	57	8	90	Aluminum	Release agent (3)	2	1.64	±0.02	0.85	0.79
TS-1	C	$[0]_{16}$	57	16	90	Aluminum	Release agent (3)	2	1.11	±0.01	0.83	0.28
TS2–2	C	$[0]_{16}$	57	16	90	Aluminum	Release agent (3)	2	1.20	±0.01	0.95	0.25
TS-2	C	$[0]_8$	57	8	90	Aluminum	Release agent (3) + FEP	2	0.92	±0.02	0.78	0.14
TS-3	C	$[0]_{16}$	57	16	90	Aluminum	Release agent (3) + FEP	2	0.79	±0.02	0.72	0.07
TS2–3	C	$[0]_{16}$	57	16	90	Aluminum	Release agent (3) + FEP	2	0.90	±0.02	0.88	0.02
TS2–4	C	$[0]_8$	57	8	90	Steel	Release agent (3)	2	1.63	±0.05	0.75	0.88
TS-4	C	$[0]_{16}$	57	16	90	Steel	Release agent (3)	2	1.15	±0.02	0.77	0.38
TS2–5	C	$[0]_{16}$	57	16	90	Steel	Release agent (3)	2	1.25	±0.02	0.88	0.37
TS-5	C	$[0]_8$	57	8	90	Steel	Release agent (3) + FEP	2	0.84	±0.04	0.65	0.19
TS-6	C	$[0]_{16}$	57	16	90	Steel	Release agent (3) + FEP	2	0.78	±0.05	0.60	0.18
TS2–6	C	$[0]_{16}$	57	16	90	Steel	Release agent (3) + FEP	2	0.85	±0.02	0.81	0.04

[a] The number within parenthesis denotes the number of coats of release agent applied. FEP denotes the use of a fluorinated ethylene propylene sheet.
[b] The range shown represents 1/2 (maximum measured value—minimum measured value).

Table A4
Experiment 4: design and results

Part ID	Part shape	Lay-up	Flange length (mm)	Thickness (plies)	Part angle (°)	Tool material	Tool surface[a]	Cure cycle (holds)	$\Delta\theta_{total}$ (°)	Range[b] (°)	$\Delta\theta_{corner}$ (°)	$\Delta\theta_{warpage}$ (°)
W-1	L	$[0]_{16}$	89	16	90	Steel	Release agent (2)	2	1.38	±0.01	0.96	0.42
W-2	C	$[0]_8$	89	8	90	Steel	Release agent (2)	2	2.13	±0.03	0.90	1.23
W-3	L	$[0]_8$	89	8	90	Aluminum	Release agent (2)	2	2.14	±0.03	1.10	1.04
W-4	L	$[0,45,-45,90]_s$	89	8	90	Steel	Release agent (2)	2	2.57	±0.02	1.32	1.25
W-5	L	$[0,45,-45,90]_s$	89	8	90	Aluminum	Release agent (2) + FEP	2	1.22	±0.03	1.00	0.22

[a] The number within parenthesis denotes the number of coats of release agent applied. FEP denotes the use of a fluorinated ethylene propylene sheet.
[b] The range shown represents 1/2 (maximum measured value—minimum measured value).

Table A5
Experiment 5: design and results

Part ID	Part shape	Lay-up	Flange length (mm)	Thickness (plies)	Part angle (°)	Tool material	Tool surface[a]	Cure cycle (holds)	$\Delta\theta_{total}$ (°)	Range[b] (°)	$\Delta\theta_{corner}$ (°)	$\Delta\theta_{warpage}$ (°)
F-1	C	$[0]_8$	89	8	45	Steel	Release agent (2) + FEP	2	0.61	±0.03	0.47	0.14
F-2	C	$[0]_8$	89	8	45	Steel	Release agent (2)	2	1.45	±0.07	0.58	0.87
F-3	L	$[0]_8$	89	8	45	Aluminum	Release agent (2)	2	1.52	±0.02	0.81	0.71
F-4	L	[0,45,−45,90]s	89	8	45	Aluminum	Release agent (2)	2	1.98	±0.02	0.76	1.22

[a] The number within parenthesis denotes the number of coats of release agent applied. FEP denotes the use of a fluorinated ethylene propylene sheet.
[b] The range shown represents 1/2 (maximum measured value—minimum measured value).

Table A6
Experiment 6: design and results

Part ID	Part shape	Lay-up	Flange length (mm)	Thickness (plies)	Part angle (°)	Tool material	Tool surface[a]	Cure cycle (holds)	$\Delta\theta_{total}$ (°)	Range[b] (°)	$\Delta\theta_{corner}$ (°)	$\Delta\theta_{warpage}$ (°)
TA-1	L	$[0]_8$	57	8	90	Aluminum	Release agent (2)	1	1.03	0.00	0.84	0.19
TA-2	L	$[0]_8$	57	8	45	Aluminum	Release agent (2)	1	0.77	0.02	0.66	0.11
TA-3	L	$[0]_8$	57	8	0	Aluminum	Release agent (2)	1	0.21	0.02	0.00	0.21
TA-4	L	$[0]_8$	57	8	90	Steel	Release agent (2)	1	0.92	0.02	0.88	0.04
TA-5	L	$[0]_8$	57	8	45	Steel	Release agent (2)	1	0.56	0.00	0.46	0.10
TA-6	L	$[0]_8$	57	8	0	Steel	Release agent (2)	1	0.13	0.01	0.01	0.13

[a] The number within parenthesis denotes the number of coats of release agent applied.
[b] The range shown represents 1/2 (maximum measured value—minimum measured value).

by approximately 0.37°. This asymmetry could be due to an uneven dispersion of release agent on the tool surface, or a possible misalignment of the fibres along one or both flanges. The other C-parts are more symmetrical, with a difference of 0.01°–0.10° between the spring-in of the two flanges. For the results presented in this study, the spring-in value indicated for C-parts represents the average value of the two flanges.

Variability between autoclave runs

A total of 10 parts were duplicated in different autoclave runs to investigate batch-to-batch variability. A difference of up to 0.27° was observed between corresponding parts cured in different autoclave runs (Table A7). The batch-to-batch variability for all the parts averaged 0.11°.

Table A7
Variability between autoclave batches

First part			Duplicate part			|Difference| (°)
Part ID	Spring-in (°)	Range (°)	Part ID	Spring-in (°)	Range (°)	
DOE-11	0.94	±0.00	DOE-11*	0.76	±0.01	0.18
DOE-12	1.00	±0.09	DOE-12*	1.04	±0.03	0.04
DOE-13	1.03	±0.06	DOE-13*	1.04	±0.10	0.01
DOE-14	1.41	±0.04	DOE-14*	1.39	±0.02	0.02
RC-6	1.89	±0.03	TS2–1	1.64	±0.02	0.25
TS-1	1.11	±0.01	TS2–2	1.20	±0.01	0.09
TS-3	0.79	±0.02	TS2–3	0.9	±0.02	0.11
RC-8	1.36	±0.02	TS2–4	1.63	±0.05	0.27
TS-4	1.15	±0.02	TS2–5	1.25	±0.02	0.10
TS-6	0.78	±0.05	TS2–6	0.85	±0.02	0.07

Duplicate parts were processed in different autoclave runs. Parts DOE-1*X** are nominally identical to parts DOE-1*X*, but made in a different autoclave run.

Table A8
Effect of moisture on spring-in (experiment 1—spring-in measurements before and after drying)

Part ID	Before drying			After drying		
	Spring-in (°)	Range (°)	Days exposed to ambient air	Spring-in (°)	Range (°)	Change in spring-in (°)
DOE-1	0.57	±0.03	64	0.65	±0.01	0.08
DOE-2	1.28	±0.06	64	1.44	±0.03	0.16
DOE-3	1.39	±0.00	15	1.41	±0.01	0.02
DOE-4	1.06	±0.08	15	1.10	±0.07	0.04
DOE-5	1.37	±0.01	15	1.37	±0.01	0.00
DOE-6	0.61	±0.07	15	0.61	±0.07	0.00
DOE-7	0.98	±0.01	64	1.09	±0.01	0.11
DOE-8	1.23	±0.18	64	1.26	±0.20	0.03
DOE-9	1.45	±0.05	42	1.51	±0.03	0.06
DOE-10	0.88	±0.02	41	0.89	±0.00	0.01
DOE-11	1.03	±0.01	43	0.94	±0.00	0.09
DOE-12	1.04	±0.00	43	1.00	±0.09	−0.04
DOE-13	0.98	±0.06	43	1.03	±0.06	0.05
DOE-14	1.37	±0.02	43	1.41	±0.04	0.04
DOE-11*	0.84	±0.04	83	0.76	±0.01	−0.08
DOE-12*	0.99	±0.02	83	1.04	±0.03	0.05
DOE-13*	0.97	±0.06	83	1.04	±0.10	0.07
DOE-14*	1.25	±0.03	83	1.39	±0.02	0.14
DOE-15	0.69	±0.04	42	0.70	±0.03	0.01
DOE-16	0.91	±0.01	41	0.91	±0.03	0.00

Effect of moisture

The effect of moisture on part shape was examined to ensure consistency of the angle measurements. After processing, the parts from experiment 1 had been exposed to ambient air from a minimum of 15 days (parts DOE-3, DOE-4, DOE-5 and DOE-6) up to a maximum of 83 days (parts DOE-11*, DOE-12*, DOE-13*, and DOE-14*) before being measured. To determine the effect of moisture absorption on spring-in, each part was measured before and after drying. The results are shown in Table A8. Drying was achieved by placing the parts inside an oven at 75±10 °C, recording their weight intermittently until the part weight had stabilized. The drying process lasted for 83 days. The parts most affected by the drying process were parts DOE-2, DOE-7, and DOE-14*. These parts showed an increase in spring-in of 0.16°, 0.11°, and 0.14° respectively after drying. These are 90° parts that were exposed to ambient air for the longest period of time prior to their measurement. This increase is consistent with Eq. (1) as moisture desorption causes through-thickness shrinkage of the laminate. Furthermore, based on Eq. (1), the increase of spring-in due to anisotropy should be greater for parts with a part angle of 90° than for parts with a part angle of 45°. The overall effect of moisture on the spring-in angle was quite small. On average, spring-in increased after drying by 0.04°, which is less than the measurement accuracy. Nevertheless, to reduce experimental error, only the measurements done on dried parts were used for the analysis of experiment 1. The parts prepared in experiments 2–6 were measured within 7 days after being processed to minimize the effect of moisture absorption.

References

[1] Radford DW, Diefendorf RJ. Shape instabilities in composites resulting from laminate anisotropy. Journal of Reinforced Plastics and Composites 1993;12:58–75.

[2] Nelson RH, Cairns DS. Prediction of dimensional changes in composite laminates during cure. Proceedings of Tomorrow's Materials: Today Society for the Advancement of Material and Process Engineering 1989:2397–410.

[3] Rennick T, Radford DW. Components of manufacturing distortion in carbon fiber/epoxy angle brackets. Proceedings of the 28th International SAMPE Technical Conference 1996:189–97.

[4] Huang CK, Yang SY. Short communication—warping in advanced composite tools with varying angles and radii. Composites Part A 1997;28A:891–3.

[5] Kim CG, Kim TW, Kim IG, Jun EJ. Spring-in deformation of composite laminated bends. Proceedings of the 7th international conference on composite materials (ICCM7) 1989:83–8.

[6] Patterson JM, Springer GS, Kollar LP. Experimental observations of the spring-in phenomenon. Proceedings of the 8th international conference on composite materials (ICCM8) 1991: 10-D-1–10-D-8.

[7] Wiersma HW, Peeters JB, Akkerman R. Prediction of springforward in continuous-fibre/polymer l shaped parts. Composites Part A 1998;29A(11):1333–42.

[8] Radford DW, Rennick T. Separating sources of manufacturing distortion in laminated composites. Journal of Reinforced Plastics and Composites 2000;19(8):621–41.

[9] Stephan A, Schwinge E, Muller J, Ory H. On the springback effect of CFRP stringers: an experimental, analytical and numerical analysis. Proceedings of the 28th International SAMPE Technical Conference 1996:245–54.

[10] Fernlund G, Rahman N, Courdji R, Bresslauer M, Poursartip A, Willden K, Nelson K. Experimental and numerical study of the effect of cure cycle, tool surface, geometry, and the lay-up on the dimensional stability of autoclave-processed composite parts. Composites Part A: Manufacturing 2002;13(3):341–51.

[11] Fernlund G, Poursartip A. the effect of tooling material, cure cycle, and tool surface finish on spring-in of autoclave procesed curved composite parts. Proceedings of the 12th International Conference on Composite Materials (ICCM12) 1999: paper 690.

[12] Johnston A, Hubert P, Fernlund G, Vaziri R, Poursartip A. Process modeling of composite structures employing a virtual autoclave concept. Science and Engineering of Composite Materials 1996;5(3–4):235–52.

[13] White SR, Hahn HT. Cure cycle optimization for the reduction of processing-induced residual stresses in composite materials. Journal of Composite Materials 1993;27(14):1352–78.

[14] Pagliuso S. Warpage, a nightmare for composite parts producers. Progress in Science and Engineering of Composites 1982:1617–23.

[15] Ridgard C. Accuracy and distortion of composite parts and tools: causes and solutions. Tooling for Composite '93 1993:93–113.

[16] Twigg GA, Poursartip A, Fernlund G. Tool-part interaction in composites processing. Proceedings of the 13th International Conference on Composite Materials (ICCM13) 2001: paper 1192.

[17] Twigg GA, Fernlund G, Poursartip A. Measurement of tool-part interfacial stress during the processing of composite laminates. Proceedings of the 16th ASC Technical Conference 2001:85–96.

[18] Twigg GA. Tool–part interaction in composites processing. MASc thesis, The University of British Columbia, 2001.

[19] Pagano NJ. Thickness expansion coefficients of composite laminates. Journal of Composite Materials 1974;8:310–2.

[20] Bogetti TA, Gillespie Jr. JW. Process-induced stress and deformation in thick-section thermoset composite laminates. Journal of Composite Materials 1992;26(5):626–59.

[21] Kim YK. Process-induced viscoelastic residual stress analysis of graphite-epoxy composite structures. PhD thesis, University of Illinois at Urbana-Champaign, 1996.

[22] Johnston A. An integrated model of the development of process induced deformation in autoclave processing of composite structures. PhD thesis, University of British Columbia, 1997.

[23] Takeda N, McCartney LN, Ogihara S. The application of a ply-refinement technique to the analysis of microscopic deformation in interlaminar-toughened laminates with transverse cracks. Composites Science and Technology 2000;60:231–40.

[24] Naji MI, Hoa SV. Curing of thick angle-bend thermoset composite part: curing process modification for uniform thickness and uniform fiber volume fraction distribution. Journal of Composite Materials 2000;34(20):1710–55.

[25] Box GEP, Hunter WG, Hunter JS. Statistics for experimenters. John Wiley & Sons, New York, 1978.